Action of Low Calcemic 1α,25-Dihydroxyvitamin D_3 Analogue EB1089 in Head and Neck Squamous Cell Carcinoma

José Prudencio, Naotake Akutsu, Naciba Benlimame, Taiqui Wang, Yolande Bastien, Roberto Lin, Martin J. Black, Moulay A. Alaoui-Jamali, John H. White

Background: **1α,25-Dihydroxyvitamin D_3 [1,25$(OH)_2D_3$] and its analogues inhibit growth of various types of cancer cells. Although the therapeutic potential of 1,25$(OH)_2D_3$ is limited by its tendency to induce hypercalcemia, analogues such as EB1089 are potent inhibitors of cell growth and exhibit reduced calcemic effects. We analyzed the antiproliferative and calcemic effects of EB1089 in tissue culture and animal models of head and neck squamous cell carcinoma (SCC) to investigate its potential as a chemotherapeutic/chemopreventive agent.** ***Methods:*** **The effects of 1,25$(OH)_2D_3$ and EB1089 on cell growth and expression of $p21^{WAF1/CIP1}$ and $p27^{KIP1}$, which encode cyclin-dependent kinase inhibitors, and a novel target, gadd45α, a growth-arrest and DNA-damage gene, were monitored in cultured murine AT-84 SCC cells. The effects of these agents on AT-84 cell growth *in vitro* and on growth of AT-84 tumors in syngeneic C3H mice were monitored; treatment started at the time of tumor implantation (early tumor model) or after 12 days (late tumor model). Weight and serum calcium levels were also monitored in these animals. All *P* values were two-sided.** ***Results:*** **Both 1,25$(OH)_2D_3$ and EB1089 arrested proliferation of AT-84 cells in G_0/G_1 phase, inhibited $p21^{WAF1/CIP1}$ expression, and induced expression of $p27^{KIP1}$ protein. 1,25$(OH)_2D_3$ also enhanced the expression of gadd45α, apparently by a p53-independent mechanism. There was a statistically significant decrease in tumor growth for 1,25$(OH)_2D_3$-treated mice ($P<.001$ for early tumor model) and EB1089-treated mice ($P<.001$ and $P = .001$ for early and late tumor models, respectively). Unlike 1,25$(OH)_2D_3$, EB1089 did not induce cachexia or hypercalcemia. The effects of 1,25$(OH)_2D_3$ and EB1089 on expression of $p21^{WAF1/CIP1}$ and GADD45α were similar in tumors and *in vitro*.** ***Conclusions:*** **EB1089 completely inhibited growth of AT-84 SCC cells at nanomolar concentrations, reduced tumor growth, and did not have calcemic effects. Our results support continued investigation of EB1089 as a chemopreventive/chemotherapeutic agent for head and neck SCC. [J Natl Cancer Inst 2001;93:745–53]**

Head and neck cancer represents a substantial burden on society. An estimated 42 800 cases of head and neck squamous cell carcinoma (SCC) occurred in the United States in 1992, with 11 600 deaths *(1).* Worldwide, more than 500 000 cases are predicted annually *(1).* While early-stage SCC of the head and neck can be treated successfully with surgery and/or radiation therapy, there remains a 3%–7% annual rate of development of second primary carcinomas *(1).* Tobacco exposure and alcohol consumption are the primary risk factors predisposing to both initial SCC and second primary carcinoma. Carcinogenesis is a multistep process, involving a continuum of genetic and cellular changes leading from premalignancy to invasive carcinoma *(2).* The high rate of second primary carcinoma has prompted a search for chemopreventive agents, defined as drugs that suppress the development of invasive cancer by inhibiting or reversing the genetic and phenotypic changes accompanying carcinogenesis *(3–5).*

Retinoids (vitamin A metabolites), the most studied class of chemopreventive agents to date, inhibit growth and stimulate differentiation of SCC *(6–13).* The primary effectors of retinoid signaling are members of the retinoic acid receptor (RARs α, β, and γ) and retinoid X receptor (RXRs α, β, and γ) families. RARs and RXRs are nuclear receptors, which function as heterodimers by binding to specific sequences in target genes known as retinoic acid response elements *(14).* Retinoids thus alter the proliferation and differentiation of target cells by regulating the expression of specific genes. Clinical trials *(7–9)* of high doses of 13-*cis*-retinoic acid (13-*cis*-RA), i.e., isotretinoin, provided evidence for a statistically significant reduction in the incidence of second primary carcinomas in treated patients as compared with control subjects. This effect diminished upon discontinuation of treatment when all sites were considered, but not in the upper aerodigestive tract alone *(8).* Furthermore, treatment was associated with clinically significant side effects, including cheilitis, dermatitis, conjunctivitis, and hypertriglyceridemia.

Given the substantial toxicity of vitamin A and its metabolites, it is important to investigate other agents that exhibit antiproliferative activity and that are potentially less toxic. The active form of vitamin D_3, 1α,25-dihydroxyvitamin D_3

Affiliations of authors: J. Prudencio, M. J. Black, Department of Otolaryngology–Head and Neck Surgery, Jewish General Hospital, Montreal, PQ, Canada; N. Akutsu, Y. Bastien, R. Lin, Department of Physiology, McGill University, Montreal; N. Benlimame, T. Wang, Montreal Centre for Experimental Therapeutics in Cancer and Lady Davis Institute for Medical Research, Montreal; M. A. Alaoui-Jamali, Department of Medicine, McGill University, Lady Davis Institute for Medical Research, and Montreal Centre for Experimental Therapeutics in Cancer; J. H. White, Departments of Physiology and Medicine, McGill University, and Montreal Centre for Experimental Therapeutics in Cancer.

Correspondence to: John H. White, Ph.D., Department of Physiology, McIntyre Medical Sciences Bldg., McGill University, 3655 Drummond St., Montreal, PQ, H3G 1Y6, Canada (e-mail: jwhite@med.mcgill.ca).

See "Notes" following "References."

[1,25$(OH)_2D_3$], has been shown to inhibit proliferation of cultured cells derived from a number of tumors *(15,16)*. Analogues of 1,25$(OH)_2D_3$ inhibit cell proliferation in *in vitro* and/or *in vivo* models of myeloid leukemia and carcinomas of the breast, prostate, and colon *(17–28)*. Signaling by 1,25$(OH)_2D_3$, which is very similar to that of retinoids, occurs through binding to specific nuclear vitamin D receptors (VDRs). The VDR functions as a heterodimer with RXRs and binds to specific vitamin D response elements (VDREs) located in the promoter regions of target genes *(3)*. Relatively few 1,25$(OH)_2D_3$ target genes have been identified to date. Transcription of the gene encoding the cyclin-dependent kinase inhibitor $p21^{WAF1/CIP1}$ in myelomonocytic cells was shown to be strongly stimulated by 1,25$(OH)_2D_3$, and its forced overexpression induced differentiation *(29,30)*. However, the magnitude of the effect of 1,25$(OH)_2D_3$ on $p21^{WAF1/CIP1}$ expression varies widely in different cell lines *(29–32)*.

The main barrier to the clinical use of 1,25$(OH)_2D_3$ has been its hypercalcemic effects. However, more than 800 analogues of 1,25$(OH)_2D_3$ have been developed in an attempt to maintain the inhibitory effect on tumor cell proliferation while reducing the potential for hypercalcemia *(33–35)*. One such analogue is EB1089, a derivative with a side chain modified to render it less susceptible to catabolic degradation. Additions include 26- and 27-dimethyl groups, an extra carbon atom at C24 (24a), and double bonds at C-22,23 and C-24 (24a) *(34,35)*. EB1089 was 60 times more potent than 1,25$(OH)_2D_3$ in inhibiting growth of MCF-7 breast cancer cells *in vitro* and 100-fold more potent than 1,25$(OH)_2D_3$ in inhibiting tumor growth by 50% in animal models of breast cancer, with only half the hypercalcemic activity *(21)*. EB1089 did not induce clinically significant hypercalcemia at doses of 0.1–1.0 μg/kg body weight per day in xenograft mouse models of human breast or prostate carcinoma *(16)*, whereas clinically significant hypercalcemia with ensuing cachexia and death was observed in mice treated with 2.5 μg/kg per day *(24,36)*.

The potent growth-inhibitory properties and potentially limited toxicity of EB1089 suggest that it may be an attractive candidate for chemotherapy/chemoprevention of head and neck SCC. This hypothesis was investigated in a series of *in vitro* and animal studies using the murine head and neck SCC line AT-84 *(37,38)*, derived from C3H mice. We compared the growth-inhibitory effects of 1,25$(OH)_2D_3$ and EB1089 *in vitro* and assessed their antitumor and calcemic activities in C3H mice implanted with AT-84 tumors. In addition, we analyzed the regulation of 1,25$(OH)_2D_3$ target genes encoding cyclin-dependent kinase inhibitors $p21^{WAF1/CIP1}$ and $p27^{KIP1}$ and a novel target, the growth-arrest and DNA-damage gene gadd45α, whose action has been associated with growth arrest and enhanced DNA repair *(39–41)*.

Materials and Methods

Nuclear Receptor Ligands and Reagents

1,25$(OH)_2D_3$ and EB1089 were supplied by Leo Laboratories (Ballerup, Denmark). 13-*cis*-RA was purchased from ICN Biomedicals (Aurora, OH). 1,25$(OH)_2D_3$, EB1089, and 13-*cis*-RA were dissolved in dimethyl sulfoxide (DMSO), and stock solutions were stored in the dark at –20 °C. Doxorubicin and cisplatin were obtained from Sigma Chemical Co. (St. Louis, MO) and David Bull Laboratories (Melbourne, Australia), respectively, and were resuspended in distilled water. Cycloheximide was purchased from Sigma Chemical Co. (Oakville, ON, Canada) and resuspended in DMSO.

Tissue Culture

The mouse SCC cell line AT-84 *(37,38,42)* was provided by Dr. Stephen E. Karp (Massey Cancer Center, Virginia Commonwealth University, Richmond, VA). The cells were cultured in RPMI-1640 medium (Life Technologies, Inc. [GIBCO BRL], Burlington, ON, Canada) plus 10% fetal bovine serum supplemented with 100 μ*M* nonessential amino acids (Life Technologies, Inc.), 1 m*M* sodium pyruvate (Life Technologies, Inc.), 2 m*M* glutamine (Life Technologies, Inc.), and 50 U/mL penicillin–streptomycin (Life Technologies, Inc.). For the analysis of the effects of 1,25$(OH)_2D_3$, EB1089, and 13-*cis*-RA on cell growth, cells were seeded in six-well plates at 15 000 cells per well in 2 mL of culture medium containing charcoal-stripped serum for 24 hours. The cells were then propagated in charcoal-stripped medium containing vehicle (DMSO) or ligand at the indicated concentrations. Medium was changed every 2 days, and fresh ligand was added as necessary. On the designated day, the cells were washed with 2 mL of phosphate-buffered saline (PBS) and removed from the plate by incubation with 0.5 mL of 0.5% trypsin–EDTA. Cell numbers were counted with the use of a hemocytometer. All treatment conditions were performed in triplicate wells. For subcutaneous injection, the cells were trypsinized and washed three times in Hanks' balanced salt solution (HBSS) (Sigma Chemical Co., Oakville, ON). Two million cells in 0.2 mL of HBSS were injected subcutaneously.

Cell Cycle Analysis

The cells were plated at a density of 1 million per 75-cm^2 flask. Twenty-four hours later, the cells were treated continuously with EB1089 at the indicated concentration for 48 hours. The cells were then collected by trypsin treatment, washed twice in PBS, and resuspended at a density of 2 million cells/mL in a solution of PBS, containing 522 mg/L spermidine trihydrochloride (Sigma Chemical Co., St. Louis), 0.5 m*M* Tris–HCl (pH 8.0), 35 μg/mL ribonuclease A, and 50 mg/mL propidium iodide. Fluorescence-activated cell sorting (FACS) analysis was performed on an Epics-Profile II flow cytometer (Beckman Coulter, Inc., Fullerton, CA), and the cell cycle distribution was determined with the use of the Multicycle Program (Pheonix Flow Systems Inc., San Diego, CA).

RNA Isolation and Northern Blotting

The cells were grown in 100-mm dishes. When appropriate, media were replaced with charcoal-stripped medium containing ligand at the indicated concentrations. Cycloheximide was added to 200 n*M* 1 hour before the addition of ligand where indicated. After incubation, total RNA was extracted with TRIZOL (Life Technologies, Inc.) according to the manufacturer's instructions. PolyA+ RNAs were isolated with the use of an Oligotex messenger RNA (mRNA) kit (QIAGEN, Valencia, CA) according to the manufacturer's instructions.

Complementary DNA probes used for northern blotting were generated by reverse transcription–polymerase chain reaction (PCR) amplification of polyA+ RNA from AT-84 cells. RNAs were reverse transcribed by oligo dT priming, and PCR amplification was performed with the use of primer sets: $p21^{WAF1/CIP1}$, 5′-GCGCGGATCCACAGCGATATCCAGACATTC-3′ and 5′-GCGGGGATCCCGTGGGCACTTCAGGG-3′; gadd45α, 5′-GGGAGGTACCCGCACTTGCAATATGAC-3′ and 5′-ATTTGGTACCGTTATTTCCATTCGGATGCC-3′; β-actin, 5′-TGTGATGGTGGGAATGGGTCAG-3′ and 5′-TTTGATGTCACGCACGCACGATTTCC-3′. Amplified fragments were subcloned into Bluescript SK+ (Stratagene, Aurora, ON, Canada) and verified by dideoxy sequencing.

For northern blotting, 20 μg of total RNA or 1 μg of polyA+ RNA was separated on a 1.0% agarose gel containing 6.3% formaldehyde, 20 m*M* 3-(*N*-morpholino)propanesulfonic acid (pH 7.0), 15 m*M* sodium acetate, and 1 m*M* EDTA. Separated RNAs were transferred to a nylon membrane (Hybond-N+; Amersham, Baie d'Urfe, Quebec, Canada). The blotted membrane was soaked in 3× standard saline citrate (SSC) (Sigma Chemical Co., St. Louis) and 0.1% sodium dodecyl sulfate (SDS) at 50 °C and prehybridized at 42 °C in 50 m*M* phosphate buffer (pH 6.5), 50% formamide, 5× SSC, and 10% Denhardt's solution containing 250 μg/mL sheared and denatured salmon sperm DNA. Hybridization was carried out in the same solution by the addition of ^{32}P-labeled complementary DNA probes. After hybridization, the membrane was washed four times in 2× SSC and 0.2% SDS for 5 minutes and three times in 0.1× SSC and 0.2% SDS for 30 minutes at 50 °C, dried, and autoradiographed.

Immunoprecipitation and Western Blotting

AT-84 cell lysates were prepared essentially as described by Hahn et al. *(43)*. After incubation, cells were washed twice with PBS, harvested by scraping in

1 mL of PBS, and centrifuged at 11 750*g* for 7 minutes at 4 °C. Pellets were resuspended in 800 μL of ice-cold lysis buffer (10 m*M* Tris–HCl [pH 7.9], 10 m*M* KCl, 1 m*M* dithiothreitol, 1.5 m*M* $MgCl_2$, and 0.5% Nonidet-P40), and cell lysates were collected by centrifugation at 11 750*g* for 10 minutes at 4 °C after 15 minutes of incubation on ice. Nuclei were pelleted, washed with Buffer A (10 m*M* Tris–HCl [pH 7.9], 10 m*M* KCl, 1 m*M* dithiothreitol, and 1.5 m*M* $MgCl_2$), resuspended in ice-cold Buffer B (50 m*M* Tris–HCl [pH 7.5], 500 m*M* KCl, 2 m*M* dithiothreitol, 5 m*M* $MgCl_2$, 0.1 m*M* EDTA, 10% sucrose, and 20% glycerol), and agitated for 1 hour at 4 °C to extract the nuclear proteins. Following centrifugation at 11 750*g* for 3 minutes at 4 °C, the supernatants were dialyzed twice with TM-1 buffer (25 m*M* Tris–HCl [pH 7.6], 100 m*M* KCl, 0.5 m*M* dithiothreitol, 5 m*M* $MgCl_2$, 0.5 m*M* EDTA, and 10% glycerol). Protease inhibitor cocktail (Boehringer Mannheim GmbH, Mannheim, Germany) was added to the above buffers immediately before use. Samples (200 μg) were immunoprecipitated at 4 °C overnight with 3 μg of anti-GADD45α (4T-27) antibody (Santa Cruz Biotechnology, Inc., Santa Cruz, CA) with 30 μL of 50% slurry protein G-Sepharose (Amersham). Beads were centrifuged at 735*g* for 3 minutes at 4 °C, and the pellets were washed four times in each lysis buffer and boiled for 3 minutes in 2× SDS–polyacrylamide gel sample buffer. Proteins were resolved by electrophoresis on a 20% polyacrylamide gel containing SDS, transferred to a nitrocellulose membrane (Hybond-C; Amersham), and probed with anti-GADD45α antibody (H-165) (Santa Cruz Biotechnology, Inc.). Western blot analyses were performed with 30 μg of total cell proteins resolved on a 20% polyacrylamide gel containing SDS. Expression of $p21^{WAF1/CIP1}$ and of $p27^{KIP1}$ was analyzed with the use of F-5 and F-8 monoclonal antibodies, respectively (Santa Cruz Biotechnology, Inc.), and p53 was detected with the use of the Ab-3 monoclonal antibody (Oncogene Research Products, Boston, MA). VDR and RXRα were detected with the use of C-20 and D-20 polyclonal antibodies, respectively (Santa Cruz Biotechnology, Inc.). Specific proteins were detected with the enhanced chemiluminescence system (NEN Life Science Products, Inc., Boston, MA).

Animal Experiments

Male syngeneic C3H mice, 6–8 weeks old, were obtained from Charles River Laboratories, St. Zotique, PQ, Canada. The mice weighed 20–24 g. All experiments were approved by the Animal Care Committee, McGill University, Montreal, Quebec. The animals were housed in cages of 10–11 and were fed standard rodent chow and water *ad libitum.* Experiment 1 was designed to evaluate the effect of EB1089 and $1,25(OH)_2D_3$ on early tumors. Thirty mice were inoculated subcutaneously with 2.0×10^6 AT-84 cells in 0.1 mL of HBSS and were randomly assigned to one of three groups, each group containing 10 animals. The groups received 0.1-mL daily intraperitoneal doses as follows: Group 1 received vehicle, group 2 was given 0.25 μg/kg EB1089, and group 3 received 0.25 μg/kg $1,25(OH)_2D_3$. In experiment 2, the mice were inoculated subcutaneously as in experiment 1. The tumors became palpable at approximately 8–10 days and could be reliably measured at 12 days. On day 12, the animals were randomly assigned to one of four groups; each group contained 11 animals. Starting on day 12, the mice received 0.1-mL daily intraperitoneal injections as follows: Group 1 received placebo vehicle, group 2 was given 0.5 μg/kg EB1089, group 3 was given 1.0 mg/kg 13-*cis*-RA, and group 4 received 1.0 mg/kg 13-*cis*-RA and 0.5 μg/kg EB1089.

Mouse weights were measured with a digital balance accurate to 0.05 g, and tumor length (*L*) and width (*W*) were measured twice weekly with the use of a caliper accurate to 0.5 mm. Tumor volume (*V*) was calculated with the use of the formula $V = L \times W \times 1/2W$. Growth was calculated as the ratio of tumor volume on a given day to initial volume. The animals that lost more than 25% of their starting weight or that showed substantial distress were killed.

After the mice were anesthetized with 0.5 mL of 2.5% Avertin (Sigma Chemical Co., St. Louis) by intraperitoneal injection, intracardial puncture was carried out to obtain 300–500 μL of blood for determinations of serum calcium and albumin levels. Blood was placed in 600-μL heparinized tubes and centrifuged at 4 °C for 10 minutes at 1500*g*. Blood serum was then separated and stored at −20 °C until analysis. Serum calcium and albumin levels were determined with the use of a spectrophotometric assay per manufacturer's instructions (Vitros Chemistry Products, Ortho-Clinical Diagnostics, Raritan, NJ). At the time that the animals were killed, their tumors were dissected and weighed. Part of the tumor was snap-frozen in liquid nitrogen, and the rest of the tumor was preserved in buffered formalin for future use.

Immunohistochemistry

Immunoperoxidase staining for $p21^{WAF1/CIP1}$ and GADD45α in formalin-fixed, paraffin-embedded tumor sections was performed by a labeled avidin–biotin method (Vector Laboratories, Inc., Burlingame, CA). Sections of tumors (6 μm) were deparaffinized in toluene and rehydrated through graded alcohol to water. Endogenous peroxidase activity was quenched by incubation in 1.5% hydrogen peroxide for 30 minutes at room temperature. Sections were immersed in 10 m*M* sodium citrate buffer (pH 6.0) and subjected to heat-induced antigen retrieval. To block binding of endogenous biotin, sections were incubated with an endogenous avidin–biotin blocking kit (Zymed Laboratories, Inc., San Francisco, CA) according to the manufacturer's instructions. To reduce nonspecific protein binding, sections were incubated with 2% goat normal serum (Jackson Laboratories, West Grove, PA) for 1 hour at room temperature. The sections were then incubated with primary antibodies: anti-$p21^{WAF1/CIP1}$ monoclonal antibody at a dilution of 1 : 100 and anti-GADD45α polyclonal antibody at a dilution of 1 : 200 (Santa Cruz Biotechnology, Inc.) overnight at 4 °C. After being rinsed extensively with PBS, the sections were incubated with the appropriate biotinylated secondary antibodies for 30 minutes at room temperature (Vector Laboratories, Inc.), followed by a 30-minute incubation with the avidin–biotin–horseradish peroxidase complex (Vector Laboratories, Inc.) in PBS and then by final color development with diaminobenzidine substrate kit peroxidase (Vector Laboratories, Inc.). Negative control experiments were performed by omission of the primary antibody. Sections were then lightly counterstained with Harris' hematoxylin (BDH Inc., Toronto, ON, Canada), dehydrated in graded alcohols, and cleared in toluene. Sections were analyzed by conventional light microscopy and photographed with the use of Kodak color slides.

Data Analysis

For *in vitro* studies, we calculated the relative growth by dividing each of the triplicate cell counts for a given concentration and day by the mean of the counts for the control wells on that day. Regression analysis was used to compare relative growth curves over time and to fit and to compare slopes for individual concentrations between groups. For *in vivo* studies in animal experiment 1, in which $1,25(OH)_2D_3$ or EB1089 treatment was initiated immediately after AT-84 cell injection, the animal weight and the corrected serum calcium measurements were compared between groups with the use of the nonparametric Kruskal–Wallis test. To analyze tumor growth, we performed an analysis of variance (ANOVA) comparing all groups, with group as an independent variable and volume as a repeated measure as a function of time. This comparison was followed up with comparisons between two groups at a time. The Greenhouse–Geisser correction factor was used to address the heterogeneity of covariances. The analysis was repeated with the use of the log of volume to reduce heterogeneity of variances and to increase the linearity. In animal experiment 2, in which EB1089 or 13-*cis*-RA treatment was initiated 12 days after the injection of AT-84 cells, we derived a relative growth measurement by dividing the volumes at each time by the initial tumor volume measured. This standardization was done to correct for any differences in tumor growth between groups before treatment was initiated. Statistical analyses were performed as in animal experiment 1. All statistical tests were two-sided and were considered to be significant at $P<.05$.

Results

Antiproliferative Effects *In Vitro* of $1,25(OH)_2D_3$ and EB1089 in Murine SCC Line AT-84

The effects of $1,25(OH)_2D_3$ and of its analogue EB1089 on proliferation of the AT-84 line *in vitro* were determined by incubation of the cells with a range of ligand concentrations over a 10-day period. Both $1,25(OH)_2D_3$ and EB1089 completely inhibited AT-84 cell growth at low nanomolar concentrations (Fig. 1, A and B). While, at concentrations of 10 n*M* or higher, there were no statistically significant differences in growth suppression between $1,25(OH)_2D_3$ and EB1089, at 1 n*M*, EB1089 showed a statistically significantly greater reduction in cell growth (*P* for difference in slopes was <.001), as shown by regression analysis of the slope of log relative growth versus time. Cell cycle analyses indicated that EB1089-treated cells

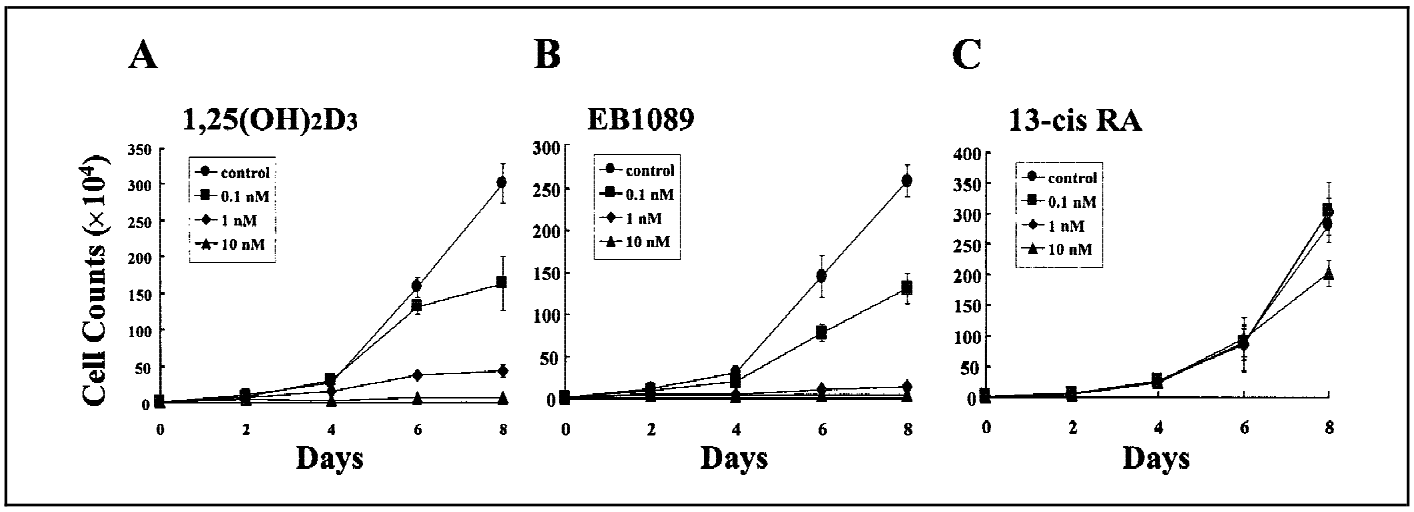

Fig. 1. Effects of 1α,25-dihydroxyvitamin D_3 (D3) (**A**), EB1089 (**B**), and 13-*cis*-retinoic acid (13-*cis*-RA) (**C**) on growth of AT-84 cells *in vitro*. Cells were grown as described in the "Materials and Methods" section and were treated with 13-*cis*- RA, D3, or EB1089 at the concentrations indicated. Cells were counted with the use of a hemocytometer. **Points** represent the mean count for an experiment run in triplicate. Statistical significance was determined with the use of regression analysis; all statistical tests are two-sided. **Error bars** represent 95% confidence intervals.

were arrested in G_0/G_1 (Table 1). Similar G_0/G_1 arrest was observed with $1,25(OH)_2D_3$-treated cells, and no evidence was found for apoptosis in cells treated with either ligand (data not shown). These results are consistent with the cytostatic effects of $1,25(OH)_2D_3$ and EB1089 in the human head and neck SCC line SCC25 (our unpublished results) and in cell lines derived from a range of other malignancies *(17,18,25,28,30)*. It is interesting that 13-*cis*-RA had no effect on AT-84 proliferation under these conditions (Fig. 1, C). This result is noteworthy because ligand-bound VDR and RARs form heterodimers with common RXR partners, and VDR/RXR and RAR/RXR heterodimers recruit common coregulatory proteins *(3,14)*.

Effects of $1,25(OH)_2D_3$ on Expression of $p21^{WAF1/CIP1}$, $p27^{KIP1}$, and gadd45α Genes in AT-84 Cells

We were interested in probing the molecular mechanisms underlying the growth-inhibitory effects of $1,25(OH)_2D_3$ in AT-84 cells. Western blotting studies revealed that the VDR and RXRα were present in AT-84 cells (Fig. 2, A). These levels were similar to those detected in the human SCC line SCC25 (data not shown). Northern blot analysis showed that treatment with $1,25(OH)_2D_3$ or with EB1089 induced expression of the endogenous 24-hydroxylase gene (Fig. 2, B), indicating that AT-84 cells express functional receptors. Previous work *(29–32)* has revealed that the gene encoding the cyclin-dependent kinase inhibitor $p21^{WAF1/CIP1}$ is a target of $1,25(OH)_2D_3$ signaling, although the magnitude of its induction varies widely among different cell types. Remarkably, we found that $1,25(OH)_2D_3$ decreases the expression of $p21^{WAF1/CIP1}$ mRNA in AT-84 cells (Fig. 2, C), representing a 50% reduction in $p21^{WAF1/CIP1}$ mRNA levels over a 48-hour period when normalized to those of actin (data not shown). Consistent with these findings, treatment with $1,25(OH)_2D_3$ also reduced $p21^{WAF1/CIP1}$ protein levels (Fig. 2, D). These results are important because they indicate that induction of $p21^{WAF1/CIP1}$ expression does not contribute to the antiproliferative effects of $1,25(OH)_2D_3$ in AT-84 cells and thus does not play an essential role in $1,25(OH)_2D_3$-dependent growth inhibition in all cell types. Our findings are also in agreement with the observation of a similar inhibitory effect of $1,25(OH)_2D_3$ on $p21^{WAF1/CIP1}$ expression in another mouse head and neck SCC model *(44)*. Treatment with $1,25(OH)_2D_3$ had no effect on the expression of the p53 protein in AT-84 cells (Fig. 2, D), in agreement with results obtained in SCC25 cells (data not shown). However, consistent with its effects on other cell types *(29–32,44)*, $1,25(OH)_2D_3$ treatment did lead to increased $p27^{KIP1}$ protein levels (Fig. 2, D).

Induction or overexpression of the growth-arrest and DNA-damage gene gadd45α has been widely associated with growth arrest *(39–41)*. The effect of $1,25(OH)_2D_3$ on gadd45α expression was analyzed by northern blotting, which revealed a gradual increase in gadd45α mRNA levels over a 48-hour period (Fig. 2, C). This effect was direct, since treatment with the protein synthesis inhibitor cycloheximide for 48 or 72 hours did not block induction (Fig. 2, C). The enhanced expression of gadd45α mRNA led to increased levels of both cytoplasmic and nuclear GADD45α proteins after 48 hours (Fig. 2, E). This result suggests that $1,25(OH)_2D_3$-dependent growth inhibition is mediated, at least in part, by enhancing the expression of GADD45α. The gadd45α gene is also a target of p53, whose activity is induced by DNA-damaging agents *(45)*. Peak levels of GADD45α induced by $1,25(OH)_2D_3$ were similar to, or somewhat less than, those induced by treatment of AT-84 cells with the DNA-damaging agents cisplatin and doxorubicin, respectively (Fig. 2, F). Unlike $1,25(OH)_2D_3$ treatment, both cisplatin

Table 1. Induction of G_0/G_1 arrest in AT-84 cells by EB1089*

	No. of cells in each phase of the cell cycle†		
	G_0/G_1	S	G_2
Control 1	37.30 (37.03 to 37.57)	54.10 (43.85 to 64.35)	8.65 (1.93 to 19.23)
EB1089	68.60 (57.77 to 79.13)	16.80 (5.98 to 27.62)	14.65 (14.24 to 15.06)

*Cells were treated with vehicle (controls) or with 0.5 μ*M* EB1089 as indicated for 48 hours and then processed for fluorescence-activated cell sorting analysis as described in the "Materials and Methods" section. Similar results were obtained with 1α,25-dihydroxyvitamin D_3.

†Values = the average (95% confidence interval) of duplicate experiments.

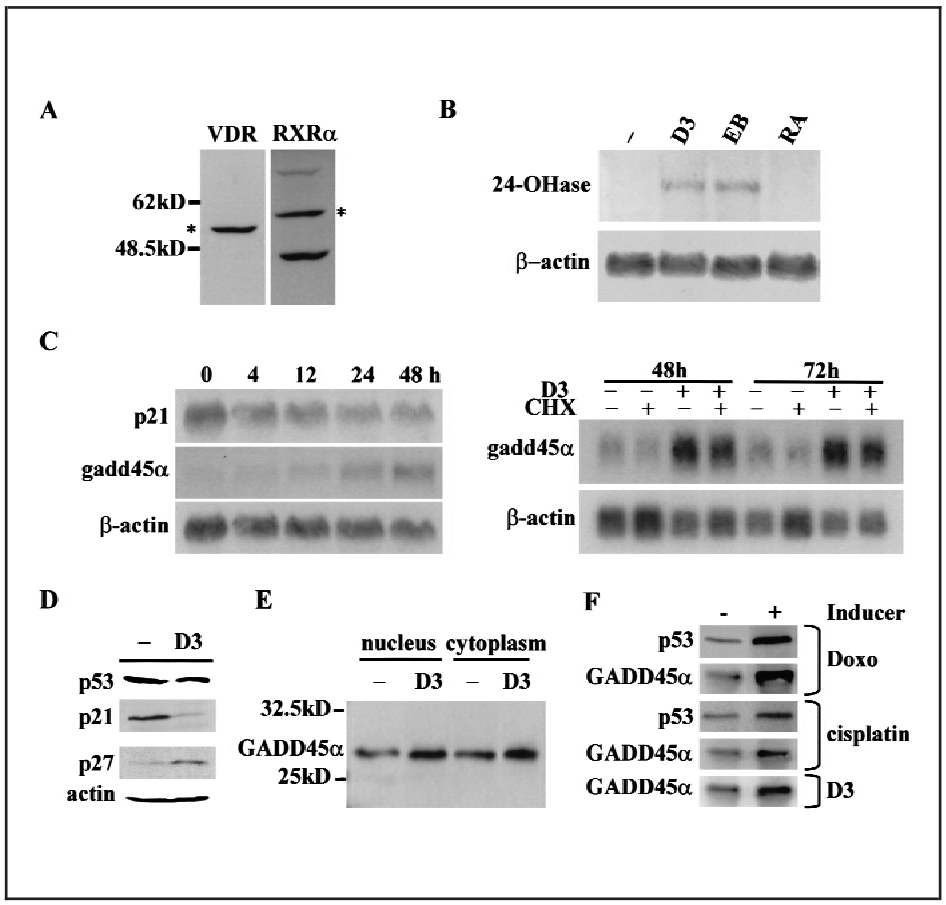

Fig. 2. Repression of $p21^{WAF1/CIP1}$ expression and induction of the growth-arrest and DNA-damage gene gadd45α in AT-84 cells under growth-inhibitory conditions. kD = kilodaltons. **A**) Western blots of retinoid X receptor α (RXRα) and vitamin D receptor (VDR) (specific bands marked with an **asterisk**). **B**) Northern blots of 24-hydroxylase (24-OHase) expression and β-actin internal control in AT-84 cells treated with vehicle (−), 1α,25-dihydroxyvitamin D_3 (D3), EB1089 (EB), or 13-*cis*-RA (RA). **C**) Northern blots (**left-hand panel**) of $p21^{WAF1/CIP1}$ (p21), gadd45α, and β-actin expression in AT-84 cells treated with D3 for the times indicated. **Right-hand panel:** induction of gadd45α messenger RNA expression over a 48-hour or 72-hour period is not blocked by cycloheximide (CHX). **D**) Typical western blots of $p21^{WAF1/CIP1}$ (p21), $p27^{KIP1}$ (p27), and p53 expression in untreated AT-84 cells and in cells treated with D3 for 48 hours. Each blot was performed three times. **E**) Expression of cytoplasmic and nuclear GADD45α protein in untreated AT-84 cells and in cells treated with 100 n*M* D3 for 48 hours. GADD45α protein was detected by immunoprecipitation, followed by western blotting. **F**) Expression of p53 and GADD45α in whole-cell extracts of AT-84 cells treated with vehicle (−), 1 μ*M* doxorubicin (doxo), or 5 μ*M* cisplatin. Expression of GADD45α in whole-cell extracts of AT-84 cells treated with vehicle (−) or D3 is provided for comparison. Expression of p53 was detected directly by western blotting of extracts, whereas GADD45α was detected by immunoprecipitation followed by western blotting.

and doxorubicin treatments increased the p53 protein levels in AT-84 cells (Fig. 2, F). Doxorubicin treatment also induced expression of $p21^{WAF1/CIP1}$ (data not shown). The lack of induction of p53 or $p21^{WAF1/CIP1}$ by $1,25(OH)_2D_3$ suggests that the observed increase in GADD45α expression occurs independently of p53. However, we cannot rule out the possibility that $1,25(OH)_2D_3$ may enhance p53 activity through post-translational mechanisms, leading to a selective effect on GADD45α expression.

Effects of EB1089 on AT-84 Tumor Growth and Serum Calcium Levels in C3H Mice

The *in vitro* experiments presented above suggest that the AT-84 cell line provides an ideal model for testing the antiproliferative effects of $1,25(OH)_2D_3$ and EB1089 *in vivo* in the syngeneic C3H mouse. Previous experiments *(38,42)* have shown that AT-84 cells form rapidly growing tumors in C3H mice. We have assessed the effects of $1,25(OH)_2D_3$ and EB1089 on tumor growth in two experimental models conducted in C3H mice inoculated with 2×10^6 AT-84 cells. Experiment 1 represents an early tumor model, in which treatment is initiated on the day of inoculation; in contrast, in experiment 2, treatment was not started until 12 days after inoculation so that tumors could become established and vascularized. We also followed animal weights and corrected serum calcium levels in experiment 1.

In experiment 1, tumor growth was followed over a 29-day period in mice treated daily with vehicle (control), $1,25(OH)_2D_3$ (0.25 μg/kg per day), or EB1089 (0.25 μg/kg per day) (Fig. 3). ANOVA with repeated measures revealed a statistically significant time effect [$F(6,19) = 59.895$; $P<.001$] and time-by-group interaction [$F(12,40) = 4.594$; $P<.001$]. This analysis was followed by comparisons between two groups at a time with the use of the Greenhouse–Geisser correction factor. Both $1,25(OH)_2D_3$ ($F = 16.5$; $P<.001$) and EB1089 ($F = 60.051$; $P<.001$) had a statistically significant effect on tumor volume when individually compared with the control, and EB1089 showed a statisti-

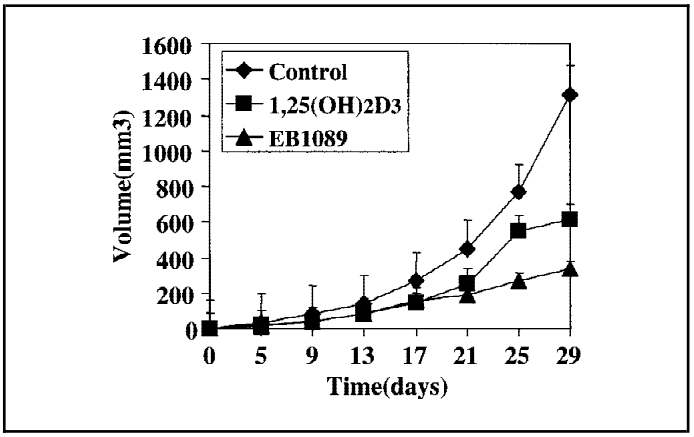

Fig. 3. Effect of EB1089 and 1α,25-dihydroxyvitamin D_3 [$1,25(OH)_2D_3$] on growth of AT-84 cells *in vivo* in an early tumor model. C3H mice received a subcutaneous injection of 2×10^6 AT-84 cells. Mice were treated with vehicle (control), $1,25(OH)_2D_3$ at a dose of 0.25 μg/kg, or EB1089 at a dose of 0.25 μg/kg via daily intraperitoneal injections starting the same day as the tumor inoculation. The length and width of the tumors were measured every 4 days, and tumor volume was calculated with the use of the following formula: length × width × (½ width). **Points** represent the mean tumor volume of surviving animals. Statistical significance was determined with the use of repeated measures analysis of variance with Greenhouse–Geisser correction factor for sphericity; all statistical tests were two-sided. **Error bars** represent 95% confidence intervals.

cally significant greater reduction in tumor volume than $1,25(OH)_2D_3$ ($F = 16.177$; $P<.001$). By day 9, the tumor volume in the control group was more than double that in either treatment group. By day 29, the mean volume in the control group had reached 1312 mm^3 (95% confidence interval [CI] = 1204 to 1420 mm^3), which was twice the mean volume in the $1,25(OH)_2D_3$-treated group (mean volume = 613 mm^3; 95% CI = 486 to 740 mm^3) and four times the mean volume in the EB1089-treated group (mean volume = 333 mm^3; 95% CI = 270 to 396 mm^3).

While $1,25(OH)_2D_3$ did result in statistically significant growth inhibition compared with the control, there was toxicity associated with its action. Four animals in this group had to be killed because of cachexia. Of the remaining animals at the completion of the experiment, the mean weights were 24.1 g, 17.0 g, and 21.6 g for the control, $1,25(OH)_2D_3$-treated, and EB1089-treated groups, respectively ($P<.001$, Kruskal–Wallis test). Corrected serum calcium levels (Fig. 4) revealed statistically significant hypercalcemia in the $1,25(OH)_2D_3$-treated group ($P = .01$, Kruskal–Wallis test), with a mean corrected serum calcium level of 3.35 mmol/L. However, there was no detectable hypercalcemia in the EB1089-treated group, with a mean corrected serum calcium level of 2.45 mmol/L, which is nearly identical to that in the control group (mean corrected serum calcium of 2.41 mmol/L).

In experiment 2, we also analyzed the effects of 13-*cis*-RA on AT-84 tumor growth to see if they were consistent with the lack of antiproliferative activity *in vitro.* Mice were randomly assigned to either treatment or control groups after 12 days of tumor growth. To correct for the differences in the mean tumor volume at this time, we present the results as growth relative to the initial measurement after randomization; the results are shown in Fig. 5. A repeated measures ANOVA showed a statistically significant time effect [$F(5,47) = 250.342$; $P<.001$] and time-by-group interaction [$F(15,147) = 4.364$; $P<.001$]. This analysis was followed by comparisons between two groups at a time with the use of the Greenhouse–Geisser correction factor. The EB1089-treated group ($F = 7.419$; $P = .001$) and

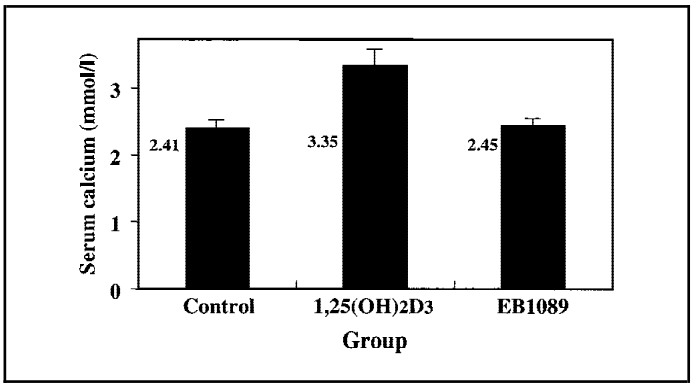

Fig. 4. Effect of EB1089 and 1α,25-dihydroxyvitamin D_3 [$1,25(OH)_2D_3$] on corrected serum calcium. Mice were treated with vehicle (control), $1,25(OH)_2D_3$ at a dose of 0.25 μg/kg, or EB1089 at a dose of 0.25 μg/kg via daily intraperitoneal injections. Blood was collected after 29 days of treatment, and serum calcium and albumin levels were determined. **Bars** represent the mean corrected serum calcium (mmol/L) per group. Serum calcium levels in $1,25(OH)_2D_3$-treated animals were statistically significantly different from those in control ($P = .01$) and EB1089-treated ($P = .03$) groups. Statistical comparisons were made with the use of the Kruskal–Wallis test. All *P* values are two-sided. **Error bars** represent 95% confidence intervals.

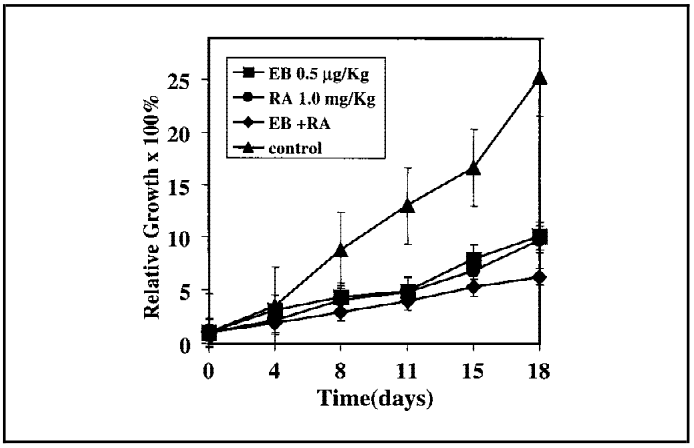

Fig. 5. Effect of EB1089 (EB), 13-*cis*-retinoic acid (RA), and combined treatment (EB + RA) on growth of AT-84 cells in an established tumor model. C3H mice received a subcutaneous injection of 2×10^6 AT-84 cells. Mice were randomly assigned to groups after 12 days of tumor growth and were treated with vehicle (control), EB at a dose of 0.5 μg/kg, RA at a dose of 1.0 mg/kg, or EB at a dose of 0.5 μg/kg combined with RA at a dose of 1.0 mg/kg (EB + RA). The length and width of the tumors were measured every 4 days, and tumor volume was calculated with the use of the following formula: length × width × (½ width). **Points** represent tumor growth relative to the mean tumor volume at the start of the injections. There were no deaths in any group. Statistical comparisons were made with the use of repeated measures analysis of variance with Greenhouse–Geisser correction factor for sphericity. All statistical tests were two-sided. **Error bars** represent 95% confidence intervals.

the group treated with EB1089 plus 13-*cis*-RA ($F = 6.082$; $P = .003$) showed a statistically significant reduction in tumor growth as compared with the control group. 13-*cis*-RA alone did not produce a statistically significant reduction in tumor growth ($F = 1.767$; $P = .179$). No statistically significant differences were found between treatment groups. After 18 days of treatment, the tumor volume in the EB1089-treated group had increased 10.1-fold, whereas the tumor volume increased 25.2-fold in the controls. Strikingly, similarly reduced tumor growth (9.8-fold) was observed in the group treated with 13-*cis*-RA (1 mg/kg per day), in spite of our observations that AT-84 cells are resistant to 13-*cis*-RA *in vitro* (Fig. 1, C). The combination of EB1089 and 13-*cis*-RA was more effective than EB1089 alone, with only a 6.3-fold increase in tumor volume. However, these differences failed to reach statistical significance. It is possible that a longer observation period may reveal statistically significant differences among treatment groups; however, large tumor volumes in the control group precluded continuation of the experiment.

Effects of EB1089 and $1,25(OH)_2D_3$ on GADD45α and $p21^{WAF1/CIP1}$ Expression in Tumors

Northern and western blot analyses showed that $1,25(OH)_2D_3$ and EB1089 directly stimulated expression of GADD45α and inhibited expression of $p21^{WAF1/CIP1}$ in AT-84 cells *in vitro* (Fig. 2). However, it is important to determine if the molecular events underlying the action of $1,25(OH)_2D_3$ and EB1089 *in vivo* are consistent with molecular analyses of their function *in vitro.* Expression levels of GADD45α and $p21^{WAF1/CIP1}$ *in vivo* were determined by immunohistochemical analyses of tumor sections from controls and animals treated with $1,25(OH)_2D_3$ or EB1089 for 29 days. These experiments revealed that GADD45α levels were elevated in tumors from $1,25(OH)_2D_3$- or EB1089-treated

animals relative to controls, whereas levels of $p21^{WAF1/CIP1}$ were decreased (Fig. 6), consistent with *in vitro* studies. Taken together, these results suggest that induction of GADD45α expression, but not of $p21^{WAF1/CIP1}$, contributes to the antiproliferative effects of $1,25(OH)_2D_3$ and EB1089 both *in vitro* and *in vivo.*

Discussion

We have been interested in both investigating the therapeutic potential of $1,25(OH)_2D_3$ analogues for treatment of head and neck SCC and understanding their underlying mechanisms of action. Early-stage primary SCCs of the head and neck (stages I and II) can be successfully treated in 60%–80% of patients. In these patients, death is more likely to be due to subsequent primary carcinomas than to recurrence of the initial lesion. Patients with more advanced disease have a poorer prognosis *(5,46,47).* These observations highlight the need for identification of chemopreventive and chemotherapeutic agents as alternatives and/or adjuncts to the established treatment modalities. Retinoids have been well studied to this end; however, their main limitation remains the substantial toxicity associated with their use and consequent poor patient compliance. In addition, their effectiveness at preventing second primary carcinoma is reversible upon discontinuation of treatment *(7,8).* While $1,25(OH)_2D_3$ also has associated toxicity due to its physiologic effect on calcium metabolism, analogues have been developed that have potent antiproliferative and differentiating effects but reduced calcemic activity. This study shows that one such analogue, EB1089, is able to inhibit growth of AT-84 murine squamous cells *in vitro* and can suppress AT-84 tumor growth *in vivo* without inducing hypercalcemia.

EB1089 is one of the most widely studied analogues of $1,25(OH)_2D_3$, with demonstrated efficacy on a wide variety of cancer cells. Our results showed that EB1089 completely inhibited growth *in vitro* of the murine head and neck SCC line AT-84 at nanomolar concentrations, inducing cell cycle arrest in G_0/G_1. Under the same conditions, 13-*cis*-RA did not statistically significantly affect proliferation of these cells. While the antiproliferative effects of $1,25(OH)_2D_3$ and its analogues are well established, the target genes mediating their effects have not yet been extensively characterized. Several investigators *(48–53)* have shown that $p21^{WAF1/CIP1}$ expression is stimulated to varying degrees during growth inhibition in cells treated with $1,25(OH)_2D_3$ or EB1089. Remarkably, we found that $p21^{WAF1/CIP1}$ mRNA and protein levels decreased under growth-inhibitory conditions in AT-84 cells. Moreover, decreased $p21^{WAF1/CIP1}$ protein levels relative to controls were observed *in vivo* in tumor sections from both $1,25(OH)_2D_3$- and EB1089-treated animals. Taken together, these results show that the antiproliferative signals induced by $1,25(OH)_2D_3$ are cell specific. While induction of $p21^{WAF1/CIP1}$ expression may be an important component of $1,25(OH)_2D_3$ signaling in some cells, our results indicate that it is not essential for $1,25(OH)_2D_3$ or its analogues to act as potent growth inhibitors.

Conversely, we found that both gadd45α mRNA and protein were induced in $1,25(OH)_2D_3$- and EB1089-treated AT-84 cells *in vitro* and that GADD45α protein levels were elevated *in vivo* in sections of tumors from $1,25(OH)_2D_3$- or EB1089-treated animals. The induction of GADD45α by $1,25(OH)_2D_3$ was comparable to that seen in AT-84 cells treated with cisplatin and doxorubucin, agents that induce GADD45α by a p53-dependent mechanism. Expression of gadd45α mRNA and protein was also enhanced in $1,25(OH)_2D_3$- and EB1089-treated human SCC25 cells *in vitro* (data not shown). The antiproliferative effects of gadd45α overexpression are well established *(39–41).* Experiments *(41)* have shown that gadd45α expression is rapidly induced in breast cancer cells overexpressing BRCA1. In addition, gene ablation studies in mice *(54)* have highlighted the role of gadd45α in maintenance of genomic stability. This finding suggests that $1,25(OH)_2D_3$ analogues may act to prevent genomic instability associated with cancer progression, as well as to block cell proliferation, supporting the notion that long-term treatment with analogues would provide a chemopreventive effect.

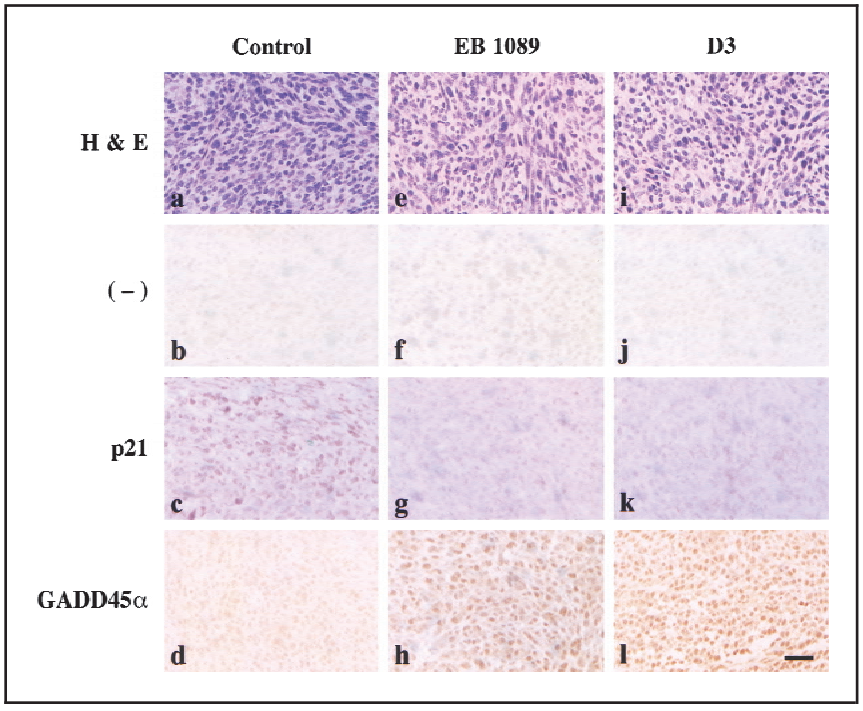

Fig. 6. Effect of EB1089 and 1α,25-dihydroxyvitamin D_3 (D3) on $p21^{WAF1/CIP1}$ (p21) and GADD45α expression in AT-84 tumors. Tumors from control animals (**a–d**), EB1089-treated animals (**e–h**), or D3-treated animals (**i–l**) were fixed, embedded in paraffin, and stained with hematoxylin–eosin (H & E) or immunolabeled for $p21^{WAF1/CIP1}$ and GADD45α. Negative control experiments (−) were performed by the omission of the primary antibodies. Results, which are typical of several sections, show decreased expression of $p21^{WAF1/CIP1}$ and increased expression of GADD45α in tumors from EB1089- or D3-treated animals compared with controls. *See* the "Materials and Methods" section for details. **Bar** = 100 μm.

Inhibition of AT-84 cell proliferation was studied *in vivo* with the use of both early and late tumor models to test whether EB1089 inhibits the growth of newly injected cells while tumor burden is low, as well as established and vascularized tumors. Tumors in EB1089-treated animals were 25%, on average, of the volume of controls in the early tumor model after 29 days and 40%, on average, of the volume of controls in the late tumor model after 18 days. There was no discernible difference in the effects of EB1089 on the two models, since tumors in treated animals were approximately 40% the volume of controls in the early model after 18 days (Fig. 3). These results are comparable to those obtained by others in breast and prostate cell lines *(17,21,23,24,27).* In addition, there was no statistically significant hypercalcemia or cachexia associated with the use of EB1089 at doses of 0.25 μg/kg per day. In contrast, 0.25 μg/kg per day of $1,25(OH)_2D_3$ resulted in the premature death of four of 10 mice and in a statistically significant weight loss in the remaining animals ($P = .001$, Kruskal–Wallis test).

It is noteworthy that 13-*cis*-RA suppressed growth of tumors *in vivo* despite resistance of AT-84 cells to its antiproliferative effects *in vitro.* This result suggests that 13-*cis*-RA may act on the tumor environment rather than on the AT-84 cells themselves. For example, Lingen et al. *(55)* have provided evidence that 13-*cis*-RA may act in an indirect fashion by inhibiting angiogenesis. It will be of interest to study the combined effects of other agents and EB1089 in the AT-84/C3H model. Other studies using EB1089 in combination with agents such as retinoids, cisplatin, paclitaxel, and tamoxifen *(56–59)* have provided evidence for combined effects.

While a full understanding of the underlying mechanisms of EB1089 action remains to be achieved, it is clearly a promising prospect as a single agent or in combination with retinoids for the treatment of head and neck SCC. A phase I trial using EB1089 in patients with advanced breast and colon cancers has been published *(60).* Maximum tolerated doses of 7 $\mu g/m^2$ (0.2 μg/kg) were estimated for prolonged treatment. In view of the mounting *in vitro* and *in vivo* evidence for the efficacy of EB1089 and the fact that there is a clear lack of alternatives for head and neck cancer patients who have failed to respond to standard treatments, a phase II trial for head and neck cancer patients represents a logical next step.

REFERENCES

(1) Vokes EE, Weichselbaum RR, Lippman SM, Hong WK. Head and neck cancer. N Engl J Med 1993;328:184–94.

(2) Slaughter DP, Southwick HW, Smejkal W. "Field cancerization" in oral stratified squamous epithelium: clinical implications of multicentric origin. Cancer 1953;6:963–8.

(3) Yu J, Papavasiliou V, Rhim J, Goltzman D, Kremer R. Vitamin D analogs: new therapeutic agents for the treatment of squamous cancer and its associated hypercalcemia. Anticancer Drugs 1995;6:101–8.

(4) Haussler MR, Haussler CA, Jurutka PW, Thompson PD, Hsieh JC, Remus LS, et al. The vitamin D hormone and its nuclear receptor: molecular actions and disease states. J Endocrinol 1997;154 Suppl:S57–73.

(5) Bikle DD. Vitamin D: new actions, new analogs, new therapeutic potential. Endocr Rev 1992;13:765–84.

(6) Lippman SM, Kessler JF, Meyskens FL. Retinoids as preventive and therapeutic anticancer agents (Part II). Cancer Treat Rep 1987;71:493–515.

(7) Lippman SM, Benner SE, Hong WK. Cancer chemoprevention. J Clin Oncol 1994;12:851–73.

(8) Hong WK, Lippman SM, Itri LM, Karp DD, Lee JS, Byers RM, et al. Prevention of second primary tumors with isotretinoin in squamous cell carcinoma of the head and neck. N Engl J Med 1990;323:795–801.

(9) Benner SE, Pajak TF, Lippman SM, Earley C, Hong WK. Prevention of second primary tumors with isotretinoin in patients with squamous cell carcinoma of the head and neck: long-term follow-up. J Natl Cancer Inst 1994;86:140–1.

(10) Pastorino U, Infante M, Maioli M, Chiesa G, Buyse M, Firket P, et al. Adjuvant treatment of stage I lung cancer with high-dose vitamin A. J Clin Oncol 1993;11:1216–22.

(11) Shalinsky DR, Bischoff ED, Lamph WW, Zhang L, Boehm MF, Davies PJ, et al. A novel retinoic acid receptor-selective retinoid, ALRT1550, has potent antitumor activity against human oral squamous cell carcinoma xenografts in nude mice. Cancer Res 1997;57:162–8.

(12) Shalinsky DR, Bischoff ED, Gregory ML, Gottardis MM, Hayes JS, Lamph WW, et al. Retinoid-induced suppression of squamous cell differentiation in human oral squamous cell carcinoma xenografts (line 1483) in athymic nude mice. Cancer Res 1995;55:3183–91.

(13) Liaudet-Coopman ED, Berchem GJ, Wellstein A. *In vivo* inhibition of angiogenesis and induction of apoptosis by retinoic acid in squamous cell carcinoma. Clin Cancer Res 1997;3:179–84.

(14) Mangelsdorf DJ, Thummel C, Beato M, Herrlich P, Schutz G, Umesono K, et al. The nuclear receptor superfamily: the second decade. Cell 1995;83:835–9.

(15) McElwain MC, Modzelewski RA, Yu WD, Russell DM, Johnson CS. Vitamin D: an antiproliferative agent with potential for therapy of squamous cell carcinoma. Am J Otolaryngol 1997;18:293–8.

(16) Kornfehl J, Formanek M, Temmel A, Knerer B, Willheim M. Antiproliferative effects of the biologically active metabolite of vitamin D_3 (1,25 $[OH]_2$ D_3) on head and neck squamous cell carcinoma. Eur Arch Otorhinolaryngol 1996;253:341–4.

(17) James SY, Mercer E, Brady M, Binderup L, Colston KW. EB1089, a synthetic analogue of vitamin D, induces apoptosis in breast cancer cells *in vivo* and *in vitro.* Br J Pharmacol 1998;125:953–62.

(18) Danielsson C, Fehsel K, Polly P, Carlberg C. Differential apoptotic response of human melanoma cells to 1 alpha,25-dihydroxyvitamin D3 and its analogues. Cell Death Differ 1998;5:946–52.

(19) Huynh H, Pollak M, Zhang JC. Regulation of insulin-like growth factor (IGF) II and IGF binding protein 3 autocrine loop in human PC-3 prostate cancer cells by vitamin D metabolite 1,25(OH)2D3 and its analog EB1089. Int J Oncol 1998;13:137–43.

(20) James SY, Williams MA, Kelsey SM, Newland AC, Colston KW. Interaction of vitamin D derivatives and granulocyte–macrophage colony-stimulating factor in leukaemic cell differentiation. Leukemia 1997;11:1017–25.

(21) VanWeelden K, Flanagan L, Binderup L, Tenniswood M, Welsh J. Apoptotic regression of MCF-7 xenografts in nude mice treated with the vitamin D3 analog, EB1089. Endocrinology 1998;139:2102–10.

(22) Xie SP, James SY, Colston KW. Vitamin D derivatives inhibit the mitogenic effects of IGF-I on MCF-7 human breast cancer cells. J Endocrinol 1997;154:495–504.

(23) Akhter J, Chen X, Bowrey P, Bolton EJ, Morris DL. Vitamin D3 analog, EB1089, inhibits growth of subcutaneous xenografts of the human colon cancer cell line, LoVo, in a nude mouse model. Dis Colon Rectum 1997;40:317–21.

(24) Lokeshwar BL, Schwartz GG, Selzer MG, Burnstein KL, Zhuang SH, Block NL, et al. Inhibition of prostate cancer metastasis *in vivo:* a comparison of 1,23-dihydroxyvitamin D (calcitriol) and EB1089. Cancer Epidemiol Biomarkers Prev 1999;8:241–8.

(25) Diaz GD, Paraskeva C, Thomas MG, Binderup L, Hague A. Apoptosis is induced by the active metabolite of vitamin D3 and its analogue EB1089 in colorectal adenoma and carcinoma cells: possible implications for prevention and therapy. Cancer Res 2000;60:2304–12.

(26) Nickerson T, Huynh H. Vitamin D analogue EB1089-induced prostate regression is associated with increased gene expression of insulin-like growth factor binding proteins. J Endocrinol 1999;160:223–9.

(27) Blutt SE, Polek TC, Stewart LV, Kattan MW, Weigel NL. A calcitriol analogue, EB1089, inhibits the growth of LNCaP tumors in nude mice. Cancer Res 2000;60:779–82.

(28) Blutt SE, Allegretto EA, Pike JW, Weigel NL. 1,25-Dihydroxyvitamin D_3 and 9-*cis*-retinoic acid act synergistically to inhibit the growth of LNCaP prostate cells and cause accumulation of cells in G1. Endocrinology 1997;138:1491–7.

(29) Liu M, Lee MH, Cohen M, Bommakanti M, Freedman LP. Transcriptional activation of the Cdk inhibitor p21 by vitamin D3 leads to the induced differentiation of the myelomonocytic cell line U937. Genes Dev 1996;10: 142–53.
(30) Munker R, Kobayashi T, Elstner E, Norman AW, Uskokovic M, Zhang W, et al. A new series of vitamin D analogs is highly active for clonal inhibition, differentiation, and induction of WAF1 in myeloid leukemia. Blood 1996;88:2201–9.
(31) Zhuang SH, Bernstein KL. Antiproliferative effect of 1α,25-dihydroxyvitamin D3 in human prostate cancer cell line LNCaP involves reduction of cyclin-dependent kinase 2 activity and persistent G1 accumulation. Endocrinology 1998;139:1197–207.
(32) Kawa S, Nikaido T, Aoki Y, Zhai Y, Kumagai T, Furihata K, et al. Vitamin D analogues up-regulate p21 and p27 during growth inhibition of pancreatic carcinoma cells. Br J Cancer 1997;76:884–9.
(33) Bouillon R, Okamura WH, Norman AW. Structure–function relationships in the vitamin D endocrine system. Endocr Rev 1995;16:200–57.
(34) Hansen CM, Maenpaa PH. EB 1089, a novel vitamin D analog with strong antiproliferative and differentiation-inducing effects on target cells. Biochem Pharmacol 1997;54:1173–9.
(35) Hansen CM, Hamberg KJ, Binderup E, Binderup L. Seocalcitol (EB 1089): a vitamin D analogue of anti-cancer potential. Background, design, synthesis, pre-clinical and clinical evaluation. Curr Pharm Des 2000;6: 803–28.
(36) Koshizuka K, Kubota T, Said J, Koike M, Binderup L, Uskokovic M, et al. Combination therapy of a vitamin D3 analog and all-*trans*-retinoic acid: effect on human breast cancer in nude mice. Anticancer Res 1999;19: 519–24.
(37) Schultz-Hector S, Haghayegh S. β-Fibroblast growth factor expression in human and murine squamous cell carcinomas and its relationship to regional endothelial cell proliferation. Cancer Res 1993;53:1444–9.
(38) Hier MP, Black MJ, Shenouda G, Sadeghi N, Karp SE. A murine model for the immunotherapy of head and neck squamous cell carcinoma. Laryngoscope 1995;105:1077–80.
(39) Papathanasiou MA, Kerr NC, Robbins JH, McBride OW, Alamo I Jr, Barrett SF, et al. Induction by ionizing radiation of the gadd45 gene in cultured human cells: lack of mediation by protein kinase C. Mol Cell Biol 1991;11:1009–16.
(40) Zhan Q, Lord KA, Alamo I Jr, Hollander MC, Carrier F, Ron D, et al. The gadd and MyD genes define a novel set of mammalian genes encoding proteins that synergistically suppress cell growth. Mol Cell Biol 1994;14: 2361–71.
(41) Harkin DP, Bean JM, Miklos D, Song YH, Truong VB, Englert C, et al. Induction of GADD45 and JNK/SAPK-dependent apoptosis following inducible expression of BRCA1. Cell 1999;97:575–86.
(42) Sadeghi N, Black MJ, Hier MP, Shenouda G, Karp SE. Generation of therapeutic T cells from draining lymph nodes in a murine model of head and neck squamous cell carcinoma. Arch Otolaryngol Head Neck Surg 1997;123:25–30.
(43) Hahn CN, Kerry DM, Omdahl JL, May BK. Identification of a vitamin D responsive element in the promoter of the rat cytochrome P450(24) gene. Nucleic Acid Res 1994;22:2410–6.
(44) Hershberger PA, Modzelewski RA, Shurin ZR, Rueger RM, Trump DL, Johnson CS. 1,25-Dihydroxycholecalciferol (1,25-D3) inhibits the growth of squamous cell carcinoma and down-modulates p21(Waf1/Cip1) *in vitro* and *in vivo.* Cancer Res 1999;59:2644–9.
(45) Levine AJ. p53, the cellular gatekeeper for growth and division. Cell 1997; 88:323–31.
(46) Lippman SM, Hong WK. Retinoid chemoprevention of upper aerodigestive tract carcinogenesis. In: DeVita VT Jr, Hellman S, Rosenberg SA, editors. Important advances in oncology. Philadelphia (PA): J. B. Lippincott; 1992. p. 93–107.
(47) Lippman SM, Hong WK. Second malignant tumors in head and neck squamous cell carcinoma: the overshadowing threat for patients with early-stage disease. Int J Radiat Oncol Biol Phys 1989;17:691–4.
(48) Wu G, Fan RS, Li W, Ko TC, Brattain MG. Modulation of cell cycle control by vitamin D3 and its analogue, EB1089, in human breast cancer cells. Oncogene 1997;15:1555–63.
(49) Park WH, Seol JG, Kim ES, Jung CW, Lee CC, Binderup L, et al. Cell cycle arrest induced by the vitamin D(3) analog EB1089 in NCI-H929 myeloma cells is associated with induction of the cyclin-dependent kinase inhibitor p27. Exp Cell Res 2000;254:279–86.
(50) Seol JG, Park WH, Kim ES, Jung CW, Binderup L, Koeffler HP, et al. Effect of a novel vitamin D3 analog, EB1089, on G1 cell cycle regulatory proteins in HL-60 cells. Int J Oncol 2000;16:315–20.
(51) Jung CW, Kim ES, Seol JG, Park WH, Lee SJ, Kim BK, et al. Antiproliferative effect of a vitamin D3 analog, EB1089, on HL-60 cells by the induction of TGF-beta receptor. Leuk Res 1999;23:1105–12.
(52) James SY, Mackay AG, Colston KW. Effects of 1,25 dihydroxyvitamin D3 and its analogues on induction of apoptosis in breast cancer cells. J Steroid Biochem Mol Biol 1996;58:395–401.
(53) Rozen F, Yang XF, Huynh H, Pollack M. Antiproliferative action of vitamin D-related compounds and insulin-like growth factor-binding protein 5 accumulation. J Natl Cancer Inst 1997;89:652–6.
(54) Hollander MC, Sheikh MS, Bulavin DV, Lundgren K, Augeri-Henmueller L, Shehee R, et al. Genomic instability in Gadd45α-deficient mice. Nat Genet 1999;23:176–84.
(55) Lingen MW, Polverini PJ, Bouck NP. Retinoic acid and interferon alpha act synergistically as antiangiogenic and antitumor agents against human head and neck squamous cell carcinoma. Cancer Res 1998;58:5551–8.
(56) Gulliford T, English J, Colston KW, Menday P, Moller S, Coombes RC. A phase I study of the vitamin D analogue EB 1089 in patients with advanced breast and colorectal cancer. Br J Cancer 1998;78:6–13.
(57) Light BW, Yu WD, McElwain MC, Russell DM, Trump DL, Johnson CS. Potentiation of cisplatin antitumor activity using a vitamin D analogue in a murine squamous cell carcinoma model system. Cancer Res 1997;57: 3759–64.
(58) Brown G, Bunce CM, Rowlands DC, Williams GR. All-*trans* retinoic acid and 1 alpha,25-dihydroxyvitamin D3 co-operate to promote differentiation of the human promyeloid leukemia cell line HL60 to monocytes. Leukemia 1994;8:806–15.
(59) Koshizuka K, Koike M, Asou H, Cho SK, Stephen T, Rude RK, et al. Combined effect of vitamin D3 analogs and paclitaxel on the growth of MCF-7 breast cancer cells *in vivo.* Breast Cancer Res Treat 1999;53: 113–20.
(60) Vink-van Wijngaarden T, Pols HA, Buurman CJ, van den Bemd GJ, Dorssers LC, Birkenhager JC, et al. Inhibition of breast cancer cell growth by combined treatment with vitamin D3 analogues and tamoxifen. Cancer Res 1994;54:5711–7.

NOTES

Supported by a grant MT-15160 from the Canadian Institutes of Health Research to J. H. White and in part by a grant from the National Cancer Institute of Canada (#010254) to M. A. Alaoui-Jamali and by funds from the Department of Otolaryngology of the Jewish General Hospital, Montreal. N. Akutsu is supported by a postdoctoral fellowship from the Royal Victoria Research Institute. J. H.White and M. A. Alaoui-Jamali are chercheurs-boursier of the Fonds de Recherche en Santé du Québec.

We thank Dr. Stephen Karp (Virginia Commonwealth University, Richmond) for the AT-84 cells, Drs. Lise Binderup and Karin Hamberg (Leo Laboratories, Ballerup, Denmark) for $1,25(OH)_2D_3$ and EB1089, and Dr. James Hanley (Department of Epidemiology and Biostatistics, McGill University, Montreal, PQ, Canada) for help with statistical analysis.

Manuscript received August 14, 2000; revised March 5, 2001; accepted March 23, 2001.